Are differences in claudin 10c isoform structure and expression associated with variation in salinity tolerance among species of killifish?

By
Adelaide Margaret von Kursell

A Thesis Submitted to
Saint Mary's University, Halifax, Nova Scotia
in Partial Fulfillment of the Requirements for
the Degree of Bachelor of Science – Honours Biology.

April 2019, Halifax, Nova Scotia

Approved: Dr. Anne Dalziel

_____
Supervisor

Approved: Dr. Genlou Sun

_____
Thesis Reader

Date: April 2019

Are differences in claudin 10c isoform structure and expression associated with variation in salinity tolerance among species of killifish?

By
Adelaide Margaret von Kursell

A Thesis Submitted to
Saint Mary's University, Halifax, Nova Scotia
in Partial Fulfillment of the Requirements for
the Degree of Bachelor of Science – Honours Biology.

April 2019, Halifax, Nova Scotia

Approved: Dr. Anne Dalziel

Supervisor

Approved: Dr. Genlou Sun

Thesis Reader

Date: April 2019

Are differences in claudin 10c isoform structure and expression associated with variation in salinity tolerance among species of killifish?

by Adelaide Margaret von Kursell

Abstract

To survive, fish must maintain ionoregulatory and osmoregulatory homeostasis during changes in environmental salinity. In hypersaline water, fish must actively excrete salts and drink water to counterbalance the passive influx of salts and efflux of water. Excess sodium ions are excreted through paracellular pathways, and the claudin proteins are core tight junction components that influence paracellular ion permeabilities. It is predicted that claudin isoform switching in osmoregulatory epithelia is critical for fish salinity acclimation. However, it is not known if the evolution of claudin structure or expression leads to differences in salinity tolerance among species of fishes. To study this question, we attempted to compare claudin isoform structure and expression in the opercular epithelia of killifishes. The Common Killifish (*Fundulus heteroclitus*) can tolerate salinities far exceeding that of full strength seawater and expresses a unique subset of claudin 10 isoforms in hypersaline conditions. The Common Killifish interbreeds with sympatric Banded Killifish (*Fundulus diaphanus*), a species that is less tolerant to high salinities, forming viable hybrid offspring, which are also less salinity tolerant. In this thesis, I aimed to test if hyper-salinity tolerance is associated with changes in claudin 10c isoform structure or expression in the operculum. In studying the expression of claudin 10c isoforms from opercular tissue, I found low concentrations of RNA, hindering my ability to study claudin expression. I was able to use gill mRNA to test for sequence variation in claudin 10c among species, and found no mutations in amino acids at functionally important sites between the Common and Banded Killifish. These results suggest that inter-specific differences in claudin 10c permeability are not the cause of differences observed in salinity tolerance between the Common Killifish and Banded Killifish.

[March 2019]

Acknowledgements

I would like to thank my supervisor Dr. Anne Dalziel for providing me the opportunity to complete my honours research in her lab. I greatly appreciate her help, guidance, enthusiasm and teaching me the true meaning behind science and scientific research. Working under Dr. Anne Dalziel's supervision has encouraged me to continue wondering about what has yet to be discovered. I thank Lauren Jonah for all her support and encouraging words throughout my research as well as for answering all my questions. I would additionally like to thank Dr. Weir and the SMU fish lab for their help, feedback and comments on my presentations, posters and writing. I am thankful to Dr. Tim Frasier and the honours class of 2018-2019 for countless peer edits and feedback throughout my thesis. Finally, I would like to thank the fish for their tissue donations.

Table of Contents

List of Figures

List of Tables

1. INTRODUCTION

1.1 Salinity change as an environmental stressor

Organisms are exposed to many stressors in their natural environments which they must cope with to survive (Schulte et al. 2007). These stressors can include changes in abiotic factors, such as temperature, pressure, pH and salinity (Osterberg et al. 2018). Changes in environmental salinity, the level of dissolved inorganic salts, is a common stressor experienced by many species of animals (Kültz et al. 2015). Organisms that can survive salinity stress must be able to detect osmotic change, and then regulate their physiology to counteract the variation to maintain optimal internal solute concentrations (Suescún-Bolívar et al. 2015). Organisms ranging from microscopic single-celled eukaryotes to multicellular metazoans actively osmoregulate to survive in environments of variable salinities (Suescún-Bolívar et al. 2015).

Fish, in particular, often experience osmotic stress because of external factors that can affect water salinity and thus profoundly influence the biochemical processes occurring in these organisms. Not all fish are able to effectively osmoregulate after a change in salinity; fish that cannot tolerate major changes in salinity are termed 'stenohaline', whereas 'euryhaline' fish are able to survive in a wide range of salinities (McCormick et al. 2013). Euryhalinity may be an evolutionary advantage for fish that often face changes in environmental salinity (Kültz et al. 2015). However, responding to these changes in salinity are extremely stressful for fish because they must counteract solute gradients by using active mechanisms to maintain a constant internal environment (homeostasis; Kültz et al. 2015).

1.2 How fish maintain osmoregulatory homeostasis

To survive, teleost fish use osmoregulatory mechanisms, such as trans or para-cellular transport of solutes, to maintain an optimal internal salt concentration despite a potentially different external salt concentration (Degnan et al. 1977). Transcellular transport is the movement of solutes through the cell, normally via channel or carrier proteins, by passing through both basolateral and apical membranes of a cell, while paracellular transport is the movement of solutes between cells, as seen in figure 1 (Günzel 2017). Ion and water transport is completed by various osmoregulatory tissues including the gills and opercular epithelium (sites of salt excretion) as well as the kidneys and bladder (aid in excretion of excess divalent ions) and intestine (absorbs water and secretes HCO_3^-) (McCormick et al. 2013). Osmoregulation is completed in these osmoregulatory tissues through specialized cells named ionocytes (McCormick et al. 2013). Ionocytes contain many transcellular transport proteins on their apical side, facing the exterior, and basolateral side, facing adjacent cells or the underlying extracellular matrix, creating a barrier to the internal blood (Degnan et al. 1977). The specific tissues, cell types and ion transporters fish use to maintain osmoregulatory homeostasis can vary between fresh water (0 ppt) saltwater (32-35 ppt) and hypersaline (>35 ppt) environments.

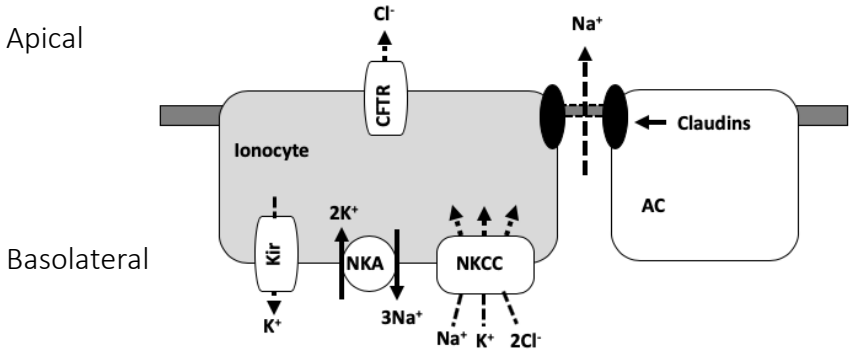

Figure 1. Diagram of the opercular or gill membrane in a high salinity environment (≥ 32 ppt). Ionocytes and accessory cells (AC) are shown with key ion channels and transporters, including the inward rectifying K^+ channel (K_{ir}), Cystic Fibrosis Transmembrane Conductance Regulator (CFTR), Na^+-K^+- ATPase (NKA) and the Na^+-K^+-Cl^--co-transporter (NKCC), and claudins, which are components of the tight junctions connecting accessory cell and ionocytes. Figure modified from Evans et al. (2005).

1.2.1 Coping with fresh water

When fish are in a hyposmotic environment, which has a decreased concentration of solutes compared to the internal concentration of the organism, the fish must actively take up salts against their concentration gradient and excrete excess water using hyperosmotic regulation (McCormick 2013). Different species of fish rely on different gill cell-types and ion transporters during fresh water acclimation (Dymowska et al. 2012). When teleost fish are moved from salt water to fresh water, focal adhesion kinase (FAK) in the gill and opercular tissue is dephosphorylated which then down regulates the activity of the Na^+-K^+-Cl^--co-transporter (NKCC) and Cystic Fibrosis Transmembrane Regulator (CFTR) in these tissues (Marshall et al. 2008, 2009). Normally, the NKCC and CFTR transporters function to transport Cl^- ions from the basolateral side of the membrane (NKCC) to the apical side of the membrane into the exterior (CFTR). During

acclimation to fresh water, NKCC and CFTR transporters decrease in activity, and allow salts to remain in the cell (Kültz et al. 2015). In addition to changes in ion transporters in freshwater acclimated fish, there is also an increased rate of ionocyte turnover and epithelial remodeling and a decrease in NaCl permeability, all of which help to further reduce passive ion loss and gain of water (Kültz et al. 2015).

1.2.2 Coping with salt water

When moving from fresh water (hyposmotic to fish blood plasma) to salt water (hyperosmotic to fish blood) the fish must excrete excess salts and retain water against their concertation gradients (Kültz et al. 2015; McCormick 2013). When the fish are first placed in a hypersaline solution, the basolateral Na^+-K^+- ATPase (NKA) will actively pump 3 Na^+ out of the ionocytes into the blood and 2 K+ into the cell, as shown in figure 1. This then allows the NKCC transporter to pump Na^+, K^+ and 2 Cl^- out of the blood into the ionocyte. Since there is now an increased concentration of salts in the cell, the CFTR transporter on the apical membrane is able to pump Cl^- out of the cell into the water. Cl^- accumulates on the external side of the membrane creating a negative membrane potential (Figure 1). The buildup of positive Na^+ ions in the blood of the fish becomes attracted to this negative membrane potential exterior to the fish. The Na^+ is then drawn out of the cell though tight junctions, which are composed of various transmembrane proteins, including claudins, occludins and junction adhesion molecules (Anderson 2001; McCormick 2003; Evans et al. 2005). To help promote water retention, the fish will actively drink, and then reabsorb water in the intestine (Kültz et al. 2015). The fish will also decrease the osmotic permeability of the gill epithelium to prevent excess ions entry (Kültz et al. 2015). In a

hypertonic environment, the fish will also increase the number of gill accessory cells and ionocytes allowing more tight junctions to form, and therefore more paracellular spaces for the Na^+ to exit the cells (Karnakey et al. 1976). The highest recorded salinity tolerance in a euryhaline fish is four times that of seawater, which was experienced by *Fundulus heteroclitus*, the Common Killifish (Kültz et al. 2015). Therefore, the Common Killifish is an ideal organism to use as a model to study tolerance to high salinities. Marshall et al. (2018) have hypothesized that the upregulation of CFTR and a set of 'hypersaline' claudin 10 isoforms that allow for increased Na^+ excretion are required for this hyper-salinity tolerance in the Common Killifish.

1.3 Hyper-salinity tolerance: The role of Claudins

Para-cellular transport is defined as transport between neighboring cells and is required to excrete ions (Na^+) in hypersaline environments (Günzel, 2016). In fish, para-cellular transport is completed through the use of adhesion proteins named claudins that are components of tight junctions (Anderson et al. 2001; Katayama et al. 2017). In humans, there are 27 members of the claudin family that are expressed throughout the body in many tissues (Katayama et al. 2017). These claudins are post-translationally regulated by phosphorylation, methylation, o-glycosylation and signaling molecules, including prostaglandins and cytokines (Awan et al. 2014; Katayama et al. 2017).

In teleost fish there have been 63 types of claudins genes discovered to date (Kolosov et al. 2013). Thirty-five of these claudins are orthologues to 17 mammalian claudins, and 21 are specific to the teleost fish lineage; the lineages of the seven remaining types of claudins are still unknown (Kolosov et al. 2013). There is thought to

be more variation in claudin proteins in fishes compared to mammals due to the polyploidization of the fish genome and many tandem gene duplications (Kolosov et al. 2013). Neofunctionalization, the duplication and gain of function of a gene, is thought to have strongly influenced the growing claudin family in teleost fish (Kolosov et al. 2013). The expression of claudins in a variety of teleost fish including the Japanese medaka, Atlantic salmon and Killifish have been tested for an association with environmental salinity. These studies determined that when fish are placed in environments with increased salinity, there is an increased expression of selected claudin isoforms, predicted to aid in sodium excretion in hypersaline environments (Tipsmark et al. 2008a; Bossus et al. 2015; Marshall et al. 2018).

1.4 Killifish as a model organism to study the evolution of salinity tolerance

Teleost fish are the largest infraclass in the class Actinopterygii, the ray-finned fishes (McCormick et al. 2013). Within this infraclass is the genus *Fundulus,* which contains 38 species (Whitehead et al. 2010). Species of *Fundulus* vary in their capacity to tolerate salinity change, but most are euryhaline (Griffith, 1974). Killifish are excellent study organisms for comparative physiologists interested in how salinity tolerance evolves because this genus is composed of species that live in different habitats with varying osmotic stressors (Whitehead et al. 2010). Therefore, we can use the comparative method to associate salinity tolerance with candidate underlying mechanisms in these closely related species. Since there is less overall variation between closely-related species than highly divergent species, any differences in underlying candidate traits are

more likely to be functionally relevant to the tolerance trait examined than in comparisons of highly divergent species (Garland et al. 2005).

Killifish live in estuaries, marshes and tidal creeks and are found along the Atlantic coast of North America ranging from Florida to Nova Scotia, as well as Bermuda, Cuba and Europe (Schulte et al. 2007; Whitehead et al. 2010). Killifish are extremely tolerant to environmental stressors, such as salinity, and have shown the ability to acclimate to changing salinities in as little as two days, making them an excellent model organism to study acclimation and adaptation to salinity (Scott et al. 2005; Giffard-Mena et al. 2007). Three co-occurring Nova Scotian species with differing salinity preferences might be a good comparative system to study the evolution of salinity tolerance; *Fundulus heteroclitus* (Common Killifish) preferring brackish or salt water, *Fundulus diaphanus (*Banded Killifish*)* preferring fresh water, and a hybrid whose preference is currently unknown (Whitehead et al. 2010).

1.4.1 Osmoregulatory mechanisms in the Killifish in salt water

The operculum

Many functional studies of killifish ionoregulatory epithelia have focused on the opercular epithelium because of the ease by which this tissue can be studied (e.g. Degnan et al. 1977; Marshall et al. 2018). Opercula are translucent bones that cover fish gills and are lined with a thin layer of epithelium that acts as a major site of osmoregulation (Degnan et al. 1977). The opercular epithelium also lines the inside of the gill chamber and contains ionocytes, and therefore can be used to study ion transport mechanisms in teleost fish (Degnan et al. 1977). The operculum is a stratified layer of epithelium

comprised of four types of cells: mucous, accessory, non-differentiated and ionocytes (Figure 2) (Degnan et al. 1977). The operculum can be used as a study tissue for ion transport because it has been shown that, when mounted, the epithelium maintains all the same properties and can actively transport ions (Degnan et al. 1977).

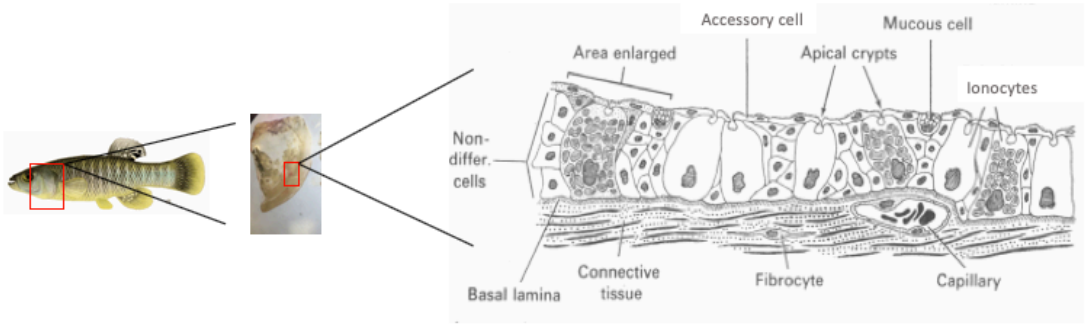

Figure 2. Killifish with indicated operculum, followed by a dissected operculum, followed by a morphological representation of cells in the opercular epithelium. Figure adapted from Figure 1 of Degnan et al. 1977.

Mechanisms contributing to opercular osmoregulation

While much is known about the ion transport capacity of the opercular epithelium, much less in known about the underlying molecular changes that occur during salinity transitions (but see Scott et al. 2005), as most molecular studies examine gill tissue. In this study I attempted to examine gene expression in the operculum to try to determine the molecular underpinnings of osmoregulatory function in this tissue. In the operculum of Killifish, as in gill, it is predicted that claudin proteins are an essential part of ion transport in hypersaline environments. In *F. heteroclitus* claudins 3, 4 and 10 have been found to be expressed in the gill and operculum (Kolosov et al. 2013). The claudin 10 family is of specific interest because they are responsive to changes in salinity and cortisol (Kolosov et al. 2013). For example, many claudin 10 isoforms are upregulated

during saltwater acclimation (Bui et al. 2014; Marshall et al. 2018). Claudin 10's are predicted to help complete the switch of the branchial epithelium from salt absorption in fresh water to salt secretion in salt water (Marshall et al. 2018).

In particular, Marshall et al. (2018), found that when Common Killifish were transferred from fresh water (0 parts per thousand, ppt) to salt water (35 ppt) higher amounts of claudin 10d and 10e isoform mRNA ('saltwater isoforms') were present in the gills. Marshall et al. (2018) then transferred fish from salt water to two times salt water (~ 60 ppt), and found that claudins 10c and 10f mRNA content ('hypersaline isoforms') significantly increased in gills, but the 'saltwater' claudin isoforms (10d and 10e) did not vary from levels measured at 35 ppt. Overall, Marshall et al. (2018) found there were salinity dependent shifts in claudin isoform expression in the Common Killifish gill at extreme salinities and proposed that claudin 10c and 10f expression are key for hypersaline tolerance (>60 ppt) in *F. heteroclitus*. Since the first extracellular loop of claudin proteins can form a pore allowing for the excretion of ions (Krause et al. 2015), Marshall et al. (2018) hypothesized that the hypersaline isoforms (10 c and f) have evolved paracellular pathway cation selectivity optimized to excrete Na^+ in hypersaline (60 ppt) conditions, based upon functional studies in the operculum. However, it is not known if these claudin isoforms (10c and10f) are highly expressed in the opercula at 60 ppt, as gene expression was measured in gill.

Variation in claudin structure

Using the *Mus musculus* claudin 15 crystal structure, Krause et al (2015), determined that the claudin pore forming site is composed of amino acids from position 31 to 66 in the

extracellular loop 1 (ECL1) region of the claudin gene (Krause et al. 2015). The ECL1 region of claudin faces the intercellular space between cells and binds to other claudin isoforms in an antiparallel or parallel fashion, and in total four or eight claudin proteins make a pore to allow for paracellular transport (Figure 3 and 7) (Suzuki et al. 2015). Marshall et al. (2018) proposed that selected mutations in the ECL1 region (positions K50, D55 and G64), of claudin 10c and f isoforms allow for increased Na^+ export in *F. heteroclitus*. Though these isoforms appear to be key in *F. heteroclitus* hyper-salinity tolerance, it is still uncertain if the same claudin isoforms are important for hyper-salinity tolerance in other species of Killifish that display reduced salinity tolerance.

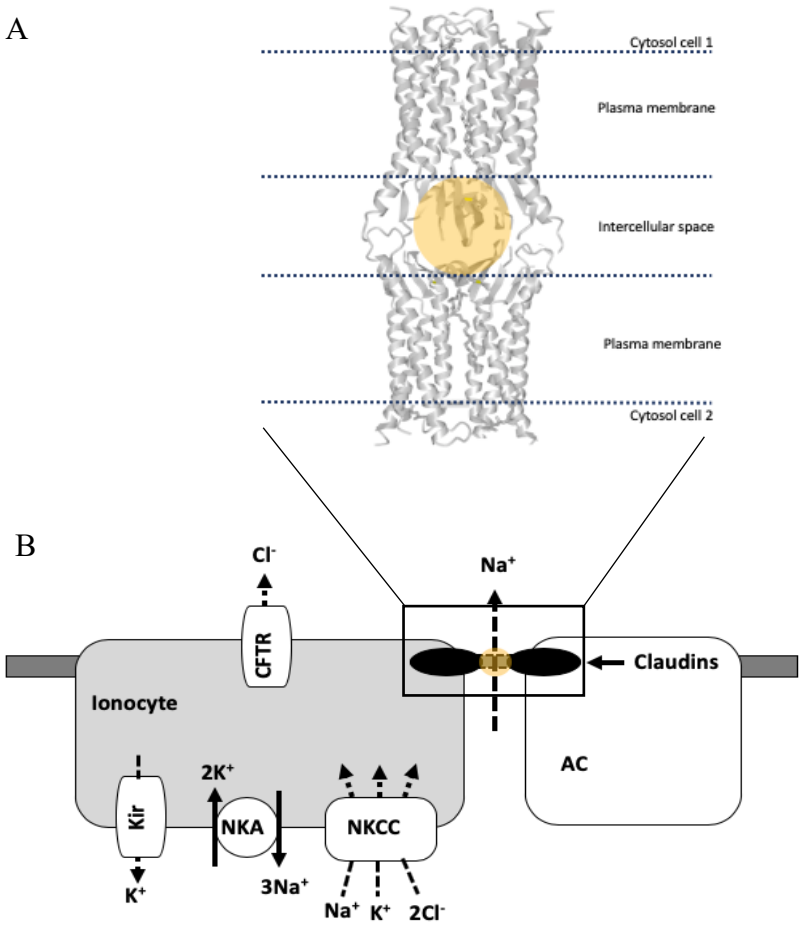

Figure 3. (A) Cartoon of the apical view of a proposed arrangement of claudins creating a pore for paracellular transport (Suzuki et al. 2015). (B) Diagram of the operculum epithelial layer consisting of an ionocyte and accessory cell (AC) with claudin proteins shown in black ovals creating the pore represented by the highlighted orange circle.

1.5 Research objectives

The first purpose of this study was to build onto the work of Marshall et al (2018), by testing if the Killifish operculum epithelium displays a similar pattern of claudin 10c and f mRNA expression at increasing salinities as the gill. I wanted to test if less hyper-salinity tolerant *Fundulus* species (i.e. Banded Killifish) also upregulated the proposed 'hypersaline' claudin isoforms (10c and 10f) at 60ppt, or if the salinity dependent gene expression of claudins 10c and 10f is unique to the more-tolerant Common Killifish. I also studied hybrids to determine if there is a correlation between hyper-salinity tolerance and claudin 10c/f expression among the three types of Killifish.

The second purpose of this study was to determine if there are functionally important differences in the first extracellular loop (ECL1) of claudin 10c between the hyper-salinity tolerant *Fundulus heteroclitus* and less hyper-salinity tolerance *Fundulus diaphanus*. This work builds on the work of Marshall et al. (2018) by providing additional information on the pore forming region in Killifishes. By testing for potential sequence variation at functionally important sites in the ECL1 region of the claudin 10c, we will be able to determine if molecular evolution of this protein could contribute to the differences in salinity tolerance seen in *F. heteroclitus* and *F. diaphanus*.

2. MATERIALS AND METHODS

2.1 Methods summary

To complete the first study objective, measuring claudin 10c and f isoform expression during hypersaline acclimation, Lauren Jonah (MSc thesis) completed a salinity tolerance experiment, acclimating Killifish to progressively higher salinities (up to 60 ppt). After acclimation, the operculum was sampled and saved for my Honours research.

To complete the second study objective, testing if there is sequence variation in the claudin 10c isoforms between all three species of Killifish, we tried to amplify parts of the claudin 10c coding regions from cDNA samples from opercular tissue. However, due to low concentrations of RNA in the opercular samples, I used gill RNA to sequence claudin coding regions instead.

2.2 Fish collection, identification and acclimation

The Common Killifish (*Fundulus heteroclitus*), Banded Killifish (*Fundulus diaphanus*) and hybrids (*F. diaphanus* x *F. heteroclitus*) used in the salinity tolerance experiment were collected from Porter's Lake, Nova Scotia (44.7433° N, 63.2972° W) by Lauren Jonah (Jonah, 2019) from May to July of 2018. Collection methods were approved by the Saint Mary's University Animal Care Committee protocols (SMU ACC AUPF 17-18) and Department of Fisheries and Oceans permit (License #343930) held by Dr. Anne Dalziel. Porter's Lake is connected to the ocean, and has a salinity range of 0-16 ppt, with salinity decreasing with increasing distance from the ocean (Mérette et al., 2009). Porter's Lake was selected for collection as all three types of Fundulus (*Fundulus heteroclitus*,

Fundulus diaphanus and F1 clonal hybrids between *F. diaphanus* and *F. heteroclitus*) live in this lake, and can be collected from the same sites in the brackish water (7.1-15.5 ppt) portion of the lake, reducing phenotypic variation that could arise due to environmental variation during early life (Dawley, 1992). In addition, the Porter's Lake Fundulus species have been well studied, and there are morphological and molecular methods to identify species (Hernandez-Chavez and Turgeon, 2007; Mérette et al. 2009; Mérette, 2009).

Both male and female fish were collected from Porter's Lake and measured by Lauren Jonah using digital Mastercraft calipers to classify species following a measuring protocol created by Mérette (2009) with a 90% accuracy rate. In addition, Svetlana Tirbhowan genotyped fish to verify morphological species classification as part of her BSc Honours Thesis.

Once collected, fish were transported to the SMU Aquarium facilities where they were acclimated to a salinity of 10 ppt, at an ambient room temperature of 18°C-20°C, and a 12 h: 12 h L:D photoperiod for at least three weeks. Fish were fed Tetra® TetraMin Tropical Flakes (Spectrum Brands, Inc., Blacksburg, VA, USA; 46% protein, 11% crude fat, 3% crude fiber, 6% moisture, 1% phosphorus, 446 mg/kg ascorbic acid, 500 mg/kg omega-3 fatty acids) in the morning, and frozen Mysis shrimp and bloodworms (at a ratio of 1-2% body mass, to satiation) in the afternoon. All experimental procedures were approved by the SMU ACC (AUPF 17-17).

2.3 Salinity tolerance experiment

To compare hyper-salinity tolerance of the Common Killifish (*Fundulus heteroclitus*), Banded Killifish (*F. diaphanus*) and F1 clonal hybrids (*F. diaphanus* x *F. heteroclitus*),

fish were gradually exposed to increasing salinities in a stepwise manner, from 10 ppt to 32 ppt to 38.5 ppt to 45 ppt to 52.5 ppt to 60 ppt (Figure 4). This salinity increase was more gradual than Marshall et al.'s (2018) procedure, as we wanted to closely monitor osmoregulatory stress in the less hyper-salinity tolerant *F. diaphanus* (Griffith, 1974). Two control groups were included for all species: 1) fish at 10 ppt sampled prior to the experiment and 2) a handling and transfer control, where the fish were handled at the same time as the treatment fish were moved to tanks with increasing salinities, but were instead transferred back to 10 ppt and measured after 24 hours has passed.

Fish were sampled at points A through E (Figure 4), by Lauren Jonah and Dr. Anne Dalziel from August 27 to September 10, 2018. Fish were euthanized in an overdose of 2g of Tricaine methanesulfonate (MS-222) buffered with 1g sodium bicarbonate ($NaHCO_3$) and immediately dissected to obtain gill and left opercula. Once sampled, opercula were wrapped in tinfoil and snap-frozen in liquid nitrogen and then stored at -80°C. This study included three to six individual samples of each of the three species of *Fundulus* (*F. heteroclitus*, *F. diaphanus* and *F. diaphanus* x *F. heteroclitus* hybrids), for each experimental group (A:10 ppt pre-experiment control, B: handling control at 10 ppt 24 hours post transfer, C: 24 hours at 32 ppt, D: 24 hours at 45 ppt and E: 24 hours at 60 ppt).

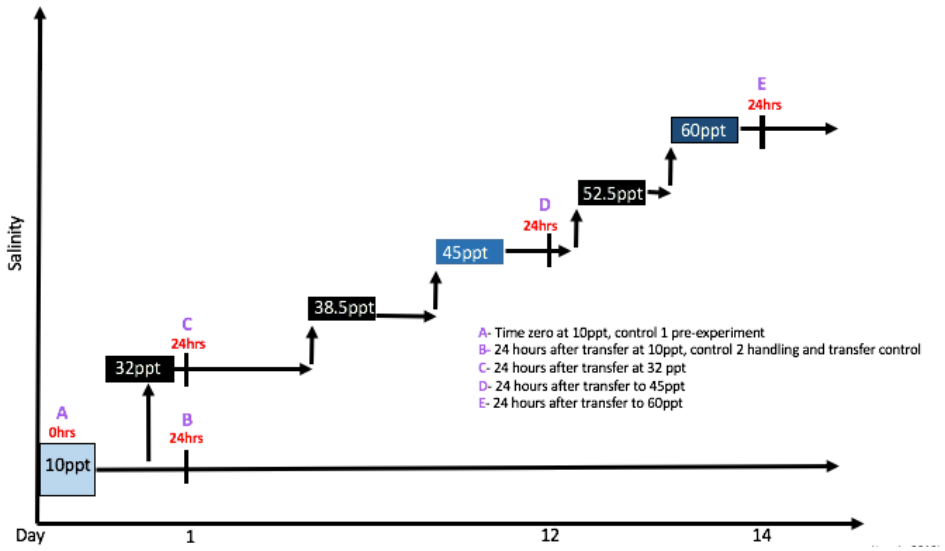

Figure 4. Diagram of the salinity tolerance experiment, including experimental and control groups, adapted from Jonah (2019). The experiment consists of a pre-experiment control group (10 ppt), a tank transfer handling control group, as well as an experimental group in increasing salinities, sampled after 24 hours of salinity exposure. Samples and samples sizes at points A to D included six *F. diaphnus*, six *F. heteroclitus*, six Hybrids, and at point E three *F. diaphnus*, six *F. heteroclitus*, five Hybrids were sampled.

2.4 RNA extraction

RNA extractions were performed on the opercular tissue using the Thermo Fisher Scientific GeneJET RNA Purification Kit (#K0731). RNA extraction was performed on all 68 samples in a randomized order, completing 12 samples at a time to prevent any confounding batch effects. Prior to starting a set of RNA extractions, all surfaces were cleaned with double distilled water and all materials used were RNase free. Additionally, gloves were worn through the experiment and changed regularly.

Samples were removed from the -80°C freezer and placed in liquid nitrogen. The opercula epithelium was dissected by scraping epithelia from the middle of the opercular bone using a scalpel into 300 µL of lysis buffer containing 2M of DL-Dithiothreitol

(Sigma Aldrich); less then 5 mg of opercula epithelia was collected per fish. The operculum tissues were then homogenized using a Kinematic rotor stator homogenizer with blade size 7mm (model GMpH), until no remaining undigested tissue was seen in tubes. The rotor stator was washed with 3 sets of double distilled water following each sample homogenization, to eliminate most residual tissue left over from previous samples. Following homogenization, the tubes were immediately placed on ice and stored at -80°C. The opercula were place in the lysis buffer within 1 minute after transfer from liquid nitrogen, and the total dissection averaged at 1:30 minutes per sample.

Following the dissections and homogenizations, tissue RNA was extracted using a GeneJET RNA purification kit, following RNA purification protocols (Thermo Scientific GeneJET RNA purification kit). Modifications to the protocol included inserting an on-column DNase treatment step, using the PureLink ™ Invitrogen kit, to eliminate genomic DNA contamination. During the wash phase (step 6) of the Gene Jet protocol, instead of adding 700 µL of wash buffer 1, 350 µL of wash buffer 1 was added to the column. This was completed to evenly distribute the additional DNase treatment step into step 6 of the GeneJet protocol, allowing the same amount of wash buffer being added to the column before and after the DNase treatment. The sample was then centrifuged at 12000 x g for 1 min to allow the wash buffer to flow through the column and bring with it any contaminants or residues on the RNA and additionally wash any remaining enzymes from the DNase treatment through the spin column. The flow through was discarded and the purification column was inserted back into the collection tube.

Extracted opercular RNA was divided into three aliquots in 1.5 mL tubes and stored in the -80°C freezer. The first aliquot contained 30 µL RNA to quantify and assess

quality on an agarose gel, the second 20 µL aliquot was for the complimentary DNA reaction and the third aliquot of 20 µL was used as a spare.

2.5 Assessment of RNA Quantity

Following RNA extractions, the samples were removed from the -80°C freezer and placed on ice to thaw. A spectrophotometer (Spectromax M3 M series Microplate Reader, Molecular Devices) was used to quantify the RNA, using Softmax Pro7 software. Using the spectra drop Absorbance RNA quantification protocol, quantification was performed by vortexing each sample, then adding 2.5 µL of sample in triplicate to the 24 well MVMP SpectraDrop TM Micro-Volume Microplate plate (Molecular Devices). RNAse free water was used in triplicates as a blank. Following the reading, the average concentration for each sample was calculated to determine the volume of sample to add to each cDNA reaction. On average, the concentration readings for opercular RNA on the spectrophotometer ranged from 2 ng/µL to 45 ng/µL.

2.6 Assessment of RNA Quality

Both RNA purity and RNA integrity were examined to test the quality of the RNA. The purity of the RNA can be determined by the $A_{260:280}$ ratios measured by the spectrophotometer. Proteins absorb at 280 nm and nucleic acids absorb at 260 nm, and ideal ratios are close to 1.8-2 which indicates good quality RNA with little protein contamination (Taylor 2010).

RNA integrity, and potential DNA contamination, was assessed by running out RNA samples on a 1% bleach gel, following the protocol by Aranda et al. (2012) and

guidelines of Taylor et al. (2010). 0.5-1ng of RNA was added per well. The gel was run at 100 volts for 1 hour using a BioRad Agarose gel electrophoresis system with 1X TAE buffer. Once the gel was complete, the BioRad Molecular Imager® Gel DocTM XR+ imaging system was used to photograph the gel under UV light. Good quality RNA should have 2 major bands (a large 28S rRNA subunit and small 18S rRNA subunits) with the larger of the bands being twice the intensity in brightness of the smaller band (Arnada et al., 2012). Image Lab™ software was then used to qualify 28S and 18S rRNA bands and calculate the ratio of ribosomal RNA.

2.7 Reverse Transcription of RNA to cDNA

After RNA quantification and quality assessment, reverse transcriptase was used to create complimentary DNA. The iScript™ cDNA Synthesis Kit and protocol (BioRad) were used to reverse transcribe the RNA. A parallel reaction also occurred to create non-reverse transcribed (NRT) samples of RNA to allow for the quantification of DNA contamination in qPCR reactions. 0.5 µL of 1.6 ng/µL RNA was added to each cDNA reaction. Final concentration of RNA in 4 µL total reaction volume was 0.23 ng/µL. cDNA samples were then stored at -20°C prior to use in qPCR reactions.

2.8 qPCR optimization

The primers used to amplify claudins 10c, d, e, f, CFTR and 18S rRNA are listed in Table 1, and are from Marshall et al (2018). All primers were first verified using BioRad qPCR guidelines (Taylor et al 2010). In particular, optimization of annealing temperatures, sample concentration, and primer concentrations were completed by Master's student

Lauren Jonah. She additionally tested efficiencies of each primer to ensure primers bind and amplify both *F. heteroclitus* and *F. diaphnus* DNA with the same efficiencies, allowing us to compare gene expression across species. Additionally, by analyzing melt curves and running the samples on an agarose gel, we confirmed that the primers produced only one product which was of the predicted size (Table 1).

Table 1. Primers used for qPCR from Marshall et al. (2018) using sequence data obtained from the National Center for Biotechnology Information (NCBI). Forward (F) primers and Reverse (R) reverse primers are noted for Claudin (cldn), cystic fibrosis transmembrane regulator (CFTR) and 18S rRNA genes.

Gene Product	**Accession no. (NCBI)**	**F/R**	**Primer sequence**	**Product size (base pairs)**
cldn-10c	XM_012873236.2	F	5'-CGCACGGAGATCACACATAC-3'	87
		R	5'-AGTCTTCCTGGTGGTGTTGG-3'	
cldn-10d	XM_012875871.2	F	5'-CGGTGATCATGTACGTGGAG-3'	85
		R	5'-TACTCTGTGGGAAGGGTGGA-3'	
cldn-10e	XM_012875869.1	F	5'-CTCTGCGGAGAAGGAGAAGA-3'	82
		R	5'-GAGAAGCTGTGGTGGGCTTA-3'	
cldn-10f	XM_012873235.2	F	5'-ACTTATATCGGCGGAGCAGA-3'	103
		R	5'-ATAAGCAGTAGGCGGCAAGA-3'	
cftr	AF000271.1	F	5'-AATCGAGCAGTTCCCAGACAAG-3'	78
		R	5'-AGCTGTTTGTGCCCATTGC-3'	
18S rRNA	M91180.1	F	5'-TTCCGATAACGAACGAGAC-3'	141
		R	5'-GACATCTAAGGGCATCACAG-3'	

2.9 qPCR

qPCR was performed to measure the mRNA content of our selected genes in the operculum (Table 1). qPCR was completed using the C1000 Touch BioRad Thermo Cycler and the SsoAdvanced™ Universal SYBR® Green Supermix from BioRad. The

cDNA was diluted in a 1/8 dilution where 0.5 µL of cDNA was added to 3.5 µL of RNAse free water. Master qPCR mix for each sample contained 0.5µL of forward primer, 0.5 µL of reverse primer and 5 µL of the SsoAdvanced™ Universal SYBR® Green Supermix. For each sample, 6 µL of qPCR master mix was added into each well with 4 µL of the given sample. The thermocycler program used followed the program used by Marshall (2018): 95°C for 10 mins, then 40 cycles of: 95°C for 30 secs (denaturing), 60°C for 60 secs (annealing and extension). The melt curve protocol was 95°C for 10 secs and then increased from 65°C to 95°C at 0.5°C at 5 second intervals. A no template control of dd H_2O was used to test for contamination and primer dimer formation. As well, a non-reverse transcribed RNA (no RT) sample was run for each sample to test for Genomic DNA contamination. Because multiple plates for each gene of interest were run, a standard curve on each plate consisting of triplicate replicates of 5 samples of a 1/5 serial dilution series was additionally run to control for between plate variability. Melt curves for each plate to monitor for random and genomic DNA contamination were also run.

Unfortunately, due to low concentrations of opercular RNA, we were not able to obtain accurate qPCR data for the opercular RNA samples.

2.10 PCR amplification of Claudin 10c from gill cDNA

To test for sequence variation in claudin 10c, we first attempted to amplify opercular cDNA to obtain claudin 10c gene products using the primers listed in Table 2. PCR was completed using the Bio Rad C1000 Touch Thermal Cycler and PCR program was as follows; 3 minutes at 95°C, 45 minutes at 95°C, 45 minutes at 60°C, 1 minute at 72°C

and finally 5 min at 72°C. However, the quantity of opercular RNA was too low for efficient amplification, so we instead obtained gill cDNA samples from the same fish from Lauren Jonah (MSc Thesis, In progress).

Table 2. Primers used for PCR and sequencing. Primers designed using data NCBI National Center for Biotechnology Information. F indicates forward sequence and R reverse. cldn represent a claudin gene.

Gene Product	**Accession no. (NCBI)**	**F/R**	**Primer sequence**	**Product size (base pairs)**
cldn-10c	XM_012873236.2	F	5'-TGCTTTGTGGTCTGCGTGG-3'	702
		R	5'-CCTGGTGGTGTTGGAGATG-3'	

Amplified PCR products were run out on 1% agarose gel to determine if a product of the correct size was amplified and were then viewed on a BioRad Molecular Imager® Gel DocTM XR+ imaging system. If bands were present, the gel was placed on a high performance UV transilluminator UVP (Ultra-Violet Products ®) and the selected bands were cut using a razor blade and placed in 1.5 ml tubes. Following gel excision, the bands from gill cDNA samples were purified using the Fisher Thermoscientific GeneJet gel extraction kit. Samples were then quantified on the Spectromax M3 M series Microplate Reader (Molecular Devices) in the same manner as for RNA samples and then sent to the Center for Applied Genomics (TCAG) at Sick Children's Hospital for Sanger sequencing in the forward and reverse direction using the primers listed in Table 2.

2.11 Claudin 10c sequencing

Following the completion of the Sanger sequencing at the Center for Applied Genomics (TCAG), chromatograms were downloaded and analysed using 4 Peaks ® software. In

this program sequences were cleaned, where the first and last 20-30 nucleotides were removed due to poor quality readings. The reverse sequence was then reversed complemented and aligned with the forward sequence in JalView to obtain a consensus sequence between the forward and reverse strands. Following the determination of a consensus sequence, Emoss transque was used to translate the nucleotide sequence into amino acid sequences. Translated sequences for all samples were then aligned to one another and additional sequences in JalView.

3. RESULTS

3.1 Opercular RNA quality and quantity

Extracted RNA was visualized by gel electrophoresis and displayed identifiable bands for the 18S and 28S ribosomal RNAs, indicating RNA was present (Figure 5). Using Image Lab to estimate the intensity of the bands, bands displayed a 2:1 ratio of 28s to 18s rRNA subunits indicating good quality RNA. However, samples were found to contain very low concentrations of RNA (≤ 2 ng/µL).

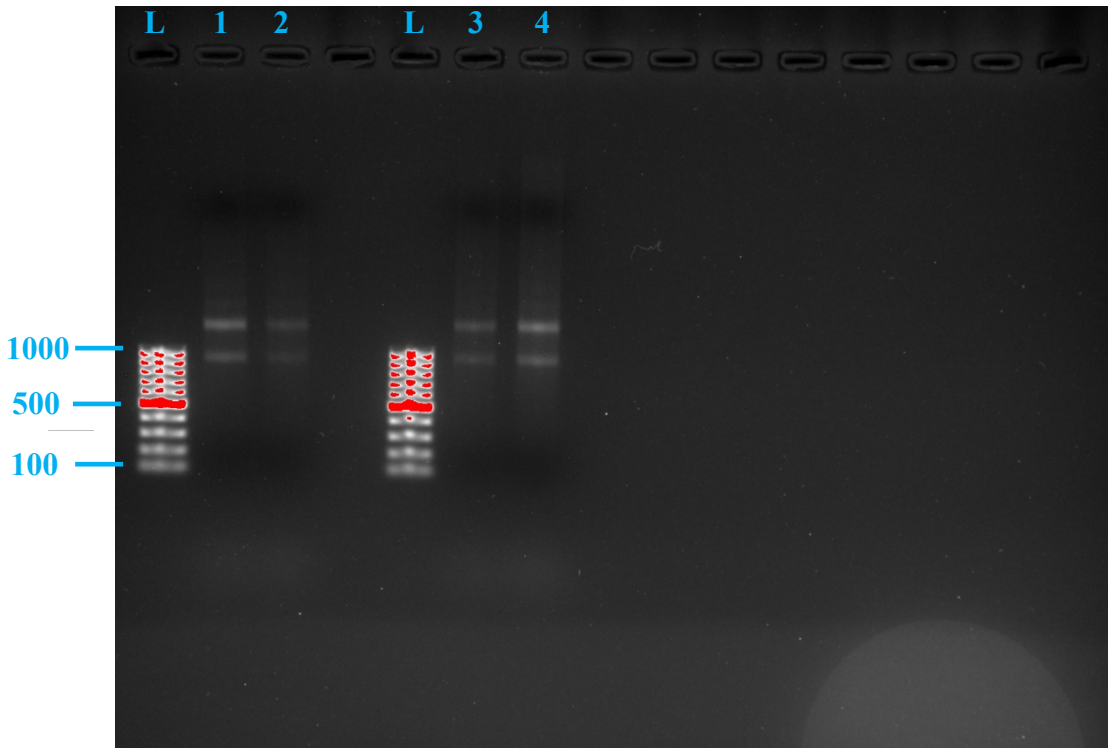

Figure 5. Bleach gel of pooled opercular RNA samples (Lanes 1-4), containing 0.5-1 ng of RNA. The top band seen is the 28S rRNA and bottom band is the 18S rRNA. This Gel includes a 100 base pair ladder (7.5 ug) (in lanes labelled L) to measure the approximate band size.

3.2 Opercular Claudin 10 isoform expression using qPCR

qPCR amplification of Claudin 10 isoforms from opercular RNA resulted in non-specific amplification (data not shown). In particular, samples did not reach a detectable level until after 25 cycles, had more than one melt peak and displayed non-specific amplification, amplifying more product in the no-template control (NTC) samples compared to reverse transcribed samples. This is predicted to be due to the low concentrations of RNA in the opercular samples, as the same qPCR primers successfully amplified claudin 10c isoforms in gill cDNA samples (Table 1). Therefore, we were not able to quantify claudin 10 isoform expression in the operculum.

3.3 PCR amplification and sequencing of the claudin 10c isoform

To obtain claudin 10c sequence information from *Fundulus heteroclitus* and *Fundulus diaphanus*, we amplified a region of claudin 10c from gill cDNA. cDNA amplification was first attempted with the RNA samples from the operculum; however, due to the low initial concentrations of RNA, this resulted in a low quantity of amplified PCR products. Since RNA samples from the gills had higher concentrations compared to the opercular samples, cDNA from the gills were amplified and these products were used to complete sequence analysis of claudin 10c.

Amplification of the ECL1 region of claudin 10c gill cDNA displayed clear single bands of the predicted size of 702 base pairs (Figure 6).

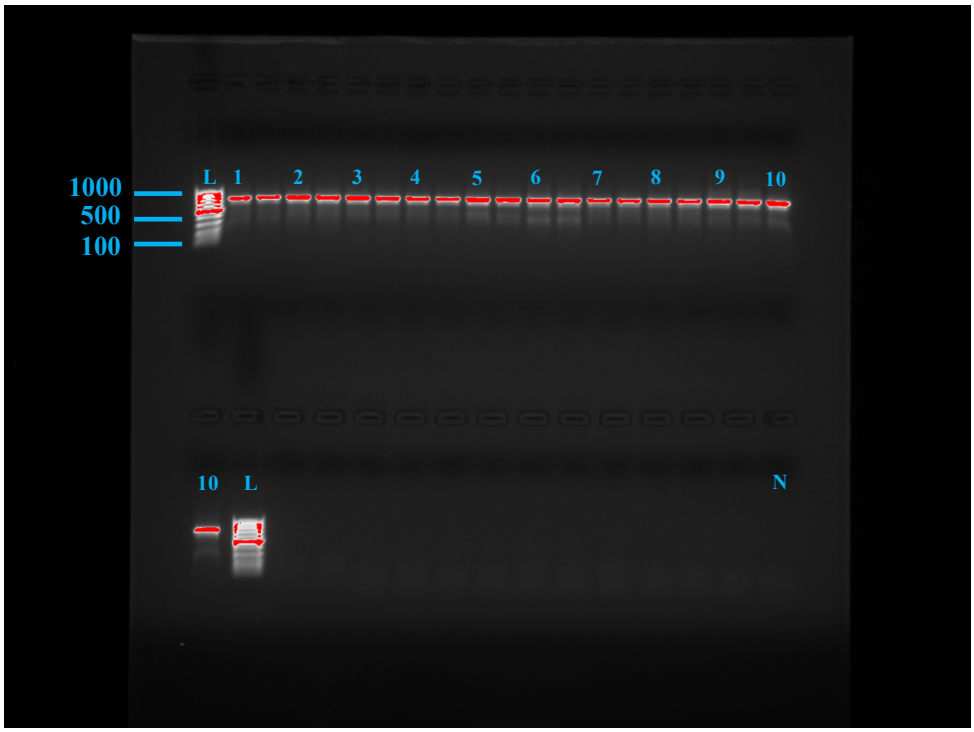

Figure 6. Claudin 10c PCR product from gill tissue cDNA. Each well contained a separate sample of PCR product either from a *Fundulus heteroclitus* or *Fundulus diaphanus*. Lane 1-5 contain *F. diaphanus* samples and lane 6-10 contain *F. heteroclitus* samples (each sample has 2 replicates run). Gel includes a 100 base pair ladder (7.5 ug) (in lanes labelled L) to measure approximate size of bands, and a negative control in lane (N). Predicted product size is 702 base pairs.

3.4 Claudin 10c sequence analysis

Claudin 10c consensus sequences were translated into amino acid sequences and aligned to reference sequences from position 31-66; the extracellular loop 1 (ECL1) region of the protein essential for claudin pore permeability and thus important for paracellular transport and sodium excretion (Krause et al. 2015). Functionally important sites of the ECL1 in pore formation found on the claudin 15 protein, for which we have an accurate protein structure, are listed in figure 7 and 8 (Krause et al. 2015). Sequences were additionally analysed at the positions proposed to influence pore formation by Marshall et al. (2018): positions K50, D55 and G64 (figure 7 and 8).

We used structural information from the published claudin 15 crystal structure (Suki et al. 2015) to predict functionally important positions in the claudin 10 protein, for which there is not yet a crystal structure available. Figure 8A displays the conservation of amino acids from claudin 15 to claudin 10c in *Fundulus heteroclitus*, supporting the use of claudin 15 as a homologous protein structure to claudin 10 isoforms.

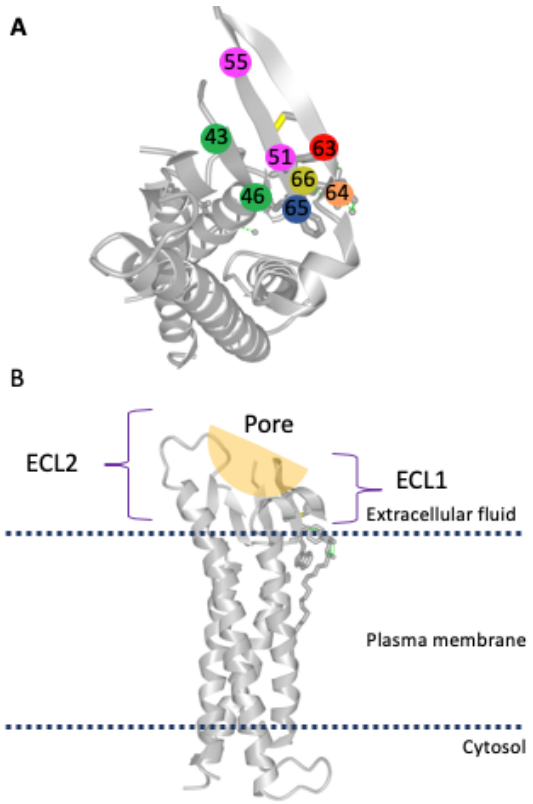

Figure 7. (A) Image representing an apical view of claudin 15, with the locations of functionally important amino acids indicated by numbered coloured dots based upon Krause et al. 2015. (B) Diagram of the lateral view of the claudin 15 protein imbedded in a plasma membrane, with the pore forming site indicated by the orange semicircle. The Claudin 15 structure was obtained from NCBI [accession number NP_001172009.1; Krause et al. 2015], and analyzed using cn3D software program.

Two mutations were found between *Fundulus diaphanus* and *Fundulus heteroclitus*, which include a Glycine to Serine mutation from *heteroclitus* to *diaphanus* in position 35, and a Serine to Alanine mutation from *heteroclitus* to *diaphanus* at position 42. However, these mutations do not change amino acid hydrophobicity and are not in positions that influence the ECL1 pore permeability (Krause et al. 2015). Additionally, these mutations did not change the charge, or drastically change the size of amino acids at positions 35 and 42.

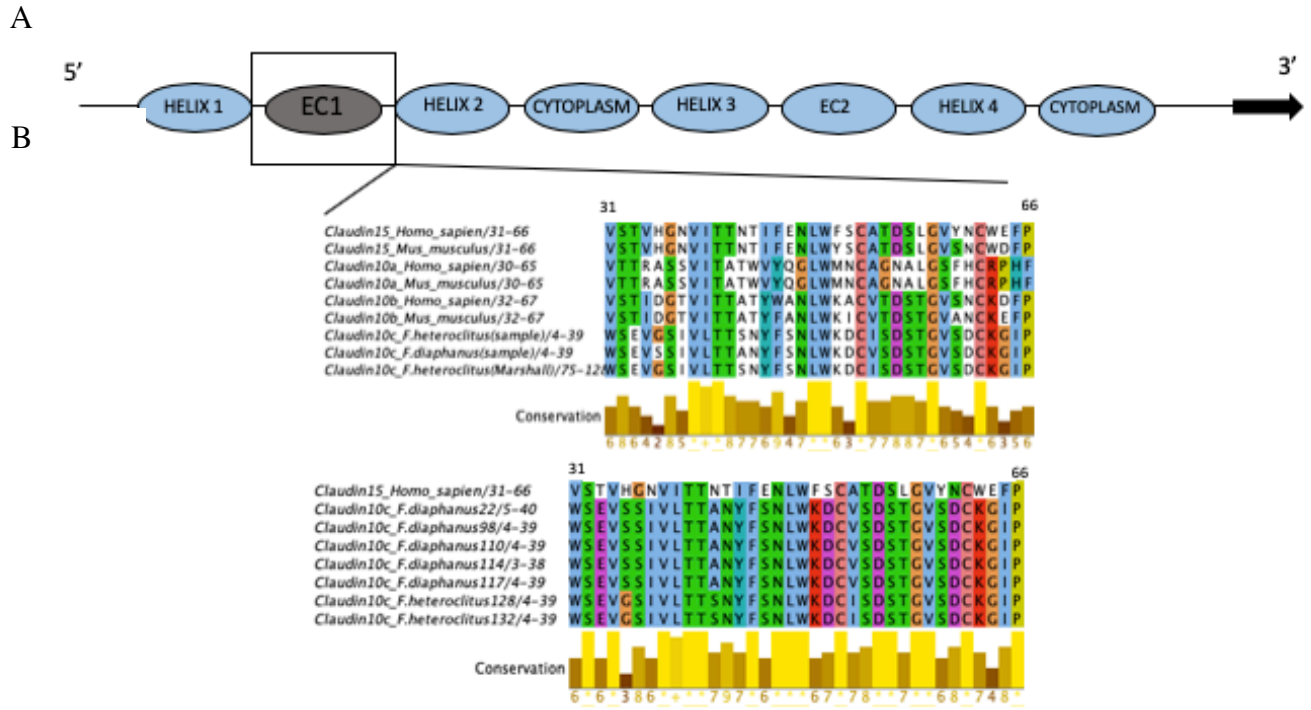

Figure 8. A) Coding regions of the claudin 15 gene adapted from Protein Data Bank [accession number NP_068365.1] (B) alignment of amino acids in the ECL1 coding region of claudin 15 and 10 from various organisms, including our samples. Figure obtained from Jalview sequencing analysis software. Accession numbers of reference sequences obtained from NCBI are as follows; Human 15 [NP_001172009.1], Mouse 15 [NP_068365.1], Human10a [NP_878268.1], Mouse 10a [NP_076367.2], Human10b [NP_008915.1], Mouse 10b [NP_067361.2], F. *heteroclitus* 10c [XM_012873236.2].

4. DISCUSSION

While carrying out my first study objective of analysing the expression of claudin 10 isoforms in the operculum, I found low concentrations of RNA and therefore could not complete this study objective. While completing my second study objective of studying sequence variation of claudin 10c in *F. heteroclitus* and *diaphanus*, I found that there exist no clear differences in amino acids sequences between the *F. heteroclitus* and *diaphanus* that are predicted to alter overall permeability or hydrophobicity of the claudin 10c protein extracellular loop 1 pore-region.

4.1 Study Objective 1: Expression of claudin 10 isoforms in the operculum

An increase in claudin 10c and f expression has been seen in the gills of the hyper-salinity tolerant *F. heteroclitus* when transferred to 60 ppt seawater (Marshal et al. 2018). My first objective was to test if claudin isoform expression also varied in the operculum with an increase in salinity in all three different species of Killifish. I was able to extract good quality RNA from the operculum, but not at a quantity high enough for qPCR amplification. Therefore, I was not able to complete my first study objective.

Preliminary results obtained from Lauren Jonah (Jonah, MSc in Applied Science student, unpublished observations) studying expression of the hypersaline claudin 10 isoforms (10c and 10f) in the gills of the three species of Killifish showed interesting trends. In particular, the less hyper-salinity tolerant *F. diaphanus* showed a slight increase in claudin 10c expression at 45 ppt, but a decrease at 60ppt. The hyper-salinity tolerant *F. heteroclitus* showed the highest level of increase in claudin 10c expression with increasing salinities, and matched the trends found by Marshall et al. (2018). The hybrids, which have an intermediate hyper-salinity tolerance, showed intermediate 10c mRNA

expression in response to hyper-salinity. Thus, these preliminary results suggest that hyper-salinity tolerance (60 ppt) is associated with the ability to upregulate claudin 10c among species of Killifish.

4.2 Study Objective 2: Sequence variation of claudin 10c in F. *heteroclitus* and *diaphanus*

The second objective of this study was to determine if there is sequence variation in the two claudin 10 'hyper-salinity' isoforms (claudin 10c and f) between the hyper-salinity tolerant *F. heteroclitus* and less-tolerant *F. diaphanus*. Due to time constraints, sequence analyses were only completed for claudin 10c.

After aligning the extracellular loop 1 (ECL1) region of five *F. diaphanus* and two *F. heteroclitus* samples (amino acid positions 31-66), I found two mutations between these species. The first mutation appeared at position 33 and was a Glycine to Serine mutation from *F. heteroclitus* to *diaphanus,* and the following mutation was at position 42 and was a Serine to Alanine mutation from *F. heteroclitus* to *diaphnus*. The two mutations between the *F. heteroclitus* and *F. diaphanus* do not change the protein's overall hydrophobicity and are not in positions that are predicted to influence ECL1 pore permeability according to Krause et al. (2015), which include the positions outlined in Figure 8. However, the mutation at position 42 from a Glycine (*F. heteroclitus)* to a serine (*F. diaphanus*) did change the hydrophobicity at the indicated position from a hydrophobic to hydrophilic amino acid.

Marshall et al (2018) built off the work of Krause et al (2015) by obtaining genomic data from a Maine Common Killifish (Reid et al. 2015) and analysing the pore

forming region of *F. heteroclitus*. The sequences we obtained for Porter's Lake *F. heteroclitus* from position 31-66 were identical to the *F. heteroclitus* sequence that Marshal et al. (2018) obtained from a fish collected from Maine, suggesting little within-species variation in this coding region. Marshall proposed a pore forming region for both 'hyper-saline' claudin isoforms of 10c and 10f (increased expression in twice the salinity of seawater). For both the 10c and 10f sequences, Marshall proposed the pore contained antiparallel alignment of sequences from position 50 to 64. To describe the important role that the pore plays in allowing the exit of ions while containing water inside the Killifish, Marshall et al. (2018) analysed interactions between these sequences. Marshall found that in both the 10c and 10f sequences, near the opening (internally) and opening (externally) there exist two ionic bonds at each end due to the attraction and charge of the given amino acids, for a total of four ionic bonds per pore forming region (Figure 9).

In the middle of the pore lies a negatively charged Aspartic acid (D) at position 55 (Figure 9). By comparing the claudin 10c and f to the claudin 10 from a *Mus musculus* where a mutation in the D65 decreased ion permeability (Laghaei et al. 2016), Marshall proposed that having two negatively charge Aspartic acids repelling each other is a critical property of the pore, creating the cation selectivity needed to conserve the internal water while excreting the excess salts in the organism (Marshall et al. 2018). Marshall et al. (2018) suggested that when an ion first enters the pore with a solvent shell intact, it is first attracted into the pore due to the pull of the ionic charges near the opening. While the ion becomes attracted to the negative charge in the middle of the pore, the water attached to the ion is released off the ion, and the ion then gets attracted towards the exterior

opening of the pore and finally to the negative charge of the exterior due to the build-up of chloride ions, leading to Na^+ excretion (Marshall et al. 2018).

Comparing all of our *F. heteroclitus* and *F. diaphanus* sequences of claudin 10c to each other and to that of the *F. heteroclitus* and *F. diaphanus* claudin 10c sequenced by Marshall (2018), I found there exist no differences in amino acids that would alter either the ionic charges at either openings of the pore or the middle negative charge created by the parallel aligned Aspartic acids at position 55, as all species had a conserved D55. This supports the previous research done by Marshall et al. (2018) that the 10c pore forming region is critical for salinity tolerance to excrete excess ions while preserving water, in not only the *F. heteroclitus* but also the less hyper-salinity tolerance *F. diaphanus* and *F. diaphanus* x *F. heteroclitus* F1 hybrids.

One difference that Marshall et al. (2018) discovered between the pore forming sequence of the claudin 10c and 10f, was that the claudin 10f contained a phenylalanine (F) at position 53, whereas the claudin 10c contained an isoleucine (I) (Figure 9). Since the claudin 10f protein is highly expressed in environments two times the salinity of seawater, Marshall et al. (2018) proposed that containing a F53 could potentially be beneficial for salt secretion in increased salinity, however the mechanism as to how this mutation is beneficial at increased salinities is still unknown.

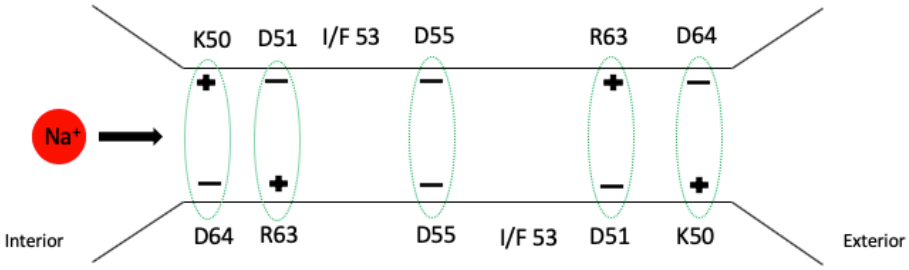

Figure 9. Claudin 10c (I53) and claudin 10f (F53) proposed pore, adapted from Marshall et al. (2018). An ion (Na+) is depicted entering the pore from the interior of the intercellular space and will exit via the pore into the exterior environment.

In summary, I found no major differences in claudin 10c structure predicted to alter the functionality of the tight junction pore between the hyper-salinity tolerant Common Killifish and less tolerant Banded Killifish. Because of this, I conclude that the evolution of claudin 10c protein function is not likely to contribute to differences in salinity tolerance in the two species of Killifish, as originally predicted. Other possible mechanisms leading to observed salinity tolerance differences among species of killifish may include differences in the expression of claudin proteins. If the hyper-salinity tolerant Common Killifish expressed an increased amount of claudin proteins compared to the less-tolerant Banded Killifish, we would predict that this trait might contribute to tolerance. Indeed, this is what is seen in the preliminary results by Lauren Jonah, as the hyper-salinity tolerant *F. heteroclitus* display the most significant increase in claudin 10c expression at 60 ppt (Jonah unpublished results).

4.3 Future studies

Future studies in this field should contribute to the first objective of this study, to test if claudin 10c and f isoform expression increases in the operculum with an increase in

salinity in three different species of Killifish and match the patterns of expression in the gill (Marshall et al. 2018). Studying the expression of claudin isoforms in the opercular epithelium is of interest as previous studies have shown that the opercular tissues also display an increase in chloride cells in hyper-saline environments, functionally similar to the response in gills (Zadunaisky et al. 1996). As well, Marshall et al. (2018) found that opercular paracellular permeability changes with acclimation from 35 to 60 ppt. mRNA should be extracted with kits specifically for extracting small amounts of RNA, for example the ThermoFisher Scientific RNAqueous TM – Micro Kit, and should additionally use both sides of the operculum to ensure adequate amounts of tissue leading into adequate concentrations of RNA samples.

To contribute to the second objective of determining if there is sequence variation in the two claudin 10 'hyper-salinity' isoforms (claudin 10c and f) between *F. heteroclitus* and *F. diaphanus* studies could include sequencing the remainder of our *F. heteroclitus* and *F. diaphanus* samples for claudin 10 f, e and d isoforms to compare to published *F. heteroclitus* information (Reid et al. 2015; Marshall et al. 2018) and test if differences in functionally important amino acids in the ECL1 region exist among the species. Completing these additional sequences of other known claudin 10 isoforms will provide information into any differences that may exists in sequences among claudin 10 isoforms of c, d, e and f that may lead to functional differences in salinity tolerance of Killifish.

The mutation at position 42 from a Glycine (*F. heteroclitus)* to a serine (*F. diaphanus*), is not currently known to be a site where mutations in amino acids would alter the overall permeability and functionality of the pore. However, site directed

mutagenesis studies would need to be conducted to verify that this mutation does not contribute to any functional differences in the claudin 10c pore among species.

Since the effect of the F53 in claudin 10f compared to the I53 in 10c is still unknown, future studies may include examining the role of each of these amino acids in pore functionality in increased salinity. Marshall et al. (2018) proposed that F53 could potentially be beneficial for salt secretion in increased salinity due to the hydrophobic bonds that F53 is capable of creating that would provide the pore an increased stability against the ionic bonds of the salt, compared to the weaker bonds that I53 would provide. An alternate hypothesis that Marshal et al. (2018) proposed was that the F53 could improve pore selectivity and therefore it would be beneficially to contain the F53 as this would mean more salt was able to exit the organism. Lastly, Marshal et al. (2018) proposed that the F53 amino acid may contribute to the shape difference between the claudin 10c and 10f pore, allowing a larger space for Na to exit, therefore making F53 beneficial in increased salinities. By completing future studies analysing the roles of these two amino acids in pore formation and functionality, additional information may be provided to the proposed mechanisms of Marshall et al. (2018).

Additional studies that may be completed to further study salinity tolerance in Killifish could include examining the expression and sequences of additional claudin isoforms other than the claudin 10's. By completing this, future researchers will be able to determine if other claudin protein are important for salinity tolerance in Killifish. Finally, by measuring the expression all tight junction genes and other changes in potentially important genes using RNA-seq, more information can be learned about the absolute quantity of claudin isoforms to determine which are most abundant in the osmoregulatory

epithelia. These studies of gene expression should be followed by measures of protein content and potential functional measures of ion transport among species to link molecular changes to osmoregulatory function.

LITERATURE CITED

Anderson, J. M. (2001). Molecular structure of tight junctions and their role in epithelial transport. *Physiology*, *16*(3), 126-130.

Aranda, P. S., LaJoie, D. M., & Jorcyk, C. L. (2012). Bleach gel: a simple agarose gel for analyzing RNA quality. *Electrophoresis*, *33*(2), 366-369.

Awan, F. M., Anjum, S., Obaid, A., Ali, A., Paracha, R. Z., & Janjua, H. A. (2014). In-silico analysis of claudin-5 reveals novel putative sites for post-translational modifications: insights into potential molecular determinants of blood–brain barrier breach during HIV-1 infiltration. *Infection, Genetics and Evolution*, *27*, 355-365.

Bio Rad iScript cDNA Synthesis Kit protocols. Philadelphia Pennsylvania, USA.

Bossus, M. C., Madsen, S. S., & Tipsmark, C. K. (2015). Functional dynamics of claudin expression in Japanese medaka (*Oryzias latipes*): response to environmental salinity. *Comparative Biochemistry and Physiology Part A: Molecular & Integrative Physiology*, *187*, 74-85.

Bui, P., & Kelly, S. P. (2014). Claudin-6,-10d, and-10e contribute to seawater acclimation in the euryhaline puffer fish *Tetraodon nigroviridis*. *Journal of Experimental Biology*, *217*, 1758-1767.

Dawley, R. M. (1992). Clonal hybrids of the common laboratory fish *Fundulus heteroclitus*. *Proceedings of the National Academy of Sciences*, *89*(6), 2485-2488.

Degnan, K. J., Karnaky Jr, K. J., & Zadunaisky, J. A. (1977). Active chloride transport in the in vitro opercular skin of a teleost (*Fundulus heteroclitus*), a gill-like epithelium rich in chloride cells. *The Journal of Physiology*, *271*(1), 155-191.

Dymowska, A. K., Hwang, P. P., & Goss, G. G. (2012). Structure and function of ionocytes in the freshwater fish gill. *Respiratory Physiology & Neurobiology*, *184*(3), 282-292.

Evans, D. H., Piermarini, P. M., & Choe, K. P. (2005). The multifunctional fish gill: dominant site of gas exchange, osmoregulation, acid-base regulation, and excretion of nitrogenous waste. *Physiological Reviews*, *85*(1), 97-177.

Fritz, E. S., & Garside, E. T. (1974a). Salinity preferences of *Fundulus heteroclitus* and *F. diaphanus* (Pisces: Cyprinodontidae): their role in geographic distribution. *Canadian Journal of Zoology*, *52*(8), 997-1003.

Fritz, E. S., & Garside, E. T. (1974b). Identification and description of hybrids of *Fundulus heteroclitus* and *F. diaphanus* (Pisces: Cyprinodontidae) from Porters Lake, Nova Scotia, with evidence for absence of backcrossing. *Canadian Journal of Zoology*, *52,* 1433-1442.

Garland, T., Bennett, A. F., & Rezende, E. L. (2005). Phylogenetic approaches in comparative physiology. *Journal of Experimental Biology*, *208*(16), 3015-3035.

Giffard-Mena, I., Boulo, V., Aujoulat, F., Fowden, H., Castille, R., Charmantier, G., & Cramb, G. (2007). Aquaporin molecular characterization in the sea-bass (*Dicentrarchus labrax*): the effect of salinity on AQP1 and AQP3 expression. *Comparative Biochemistry and Physiology Part A: Molecular & Integrative Physiology*, *148*(2), 430-444.

Griffith, R. W. (1974). Environment and salinity tolerance in the genus Fundulus. *Copeia*, 319-331.

Günzel, D. (2017). Claudins: vital partners in transcellular and paracellular transport coupling. *Pflügers Archiv-European Journal of Physiology*, *469*(1), 35-44.

Jonah, L. J. (2019). Evolutionary variation in salinity tolerance among species of killifish. MSc Thesis in Applied Science, In progress, Saint Mary's University.

Katayama, A., Handa, T., Komatsu, K., Togo, M., Horiguchi, J., Nishiyama, M., & Oyama, T. (2017). Expression patterns of claudins in patients with triple-negative breast cancer are associated with nodal metastasis and worse outcome. *Pathology International*, *67*(8), 404-413.

Karnaky, K. J., Kinter, L. B., Kinter, W. B., & Stirling, C. E. (1976). Teleost chloride cell. II. Autoradiographic localization of gill Na, K-ATPase in killifish *Fundulus heteroclitus* adapted to low and high salinity environments. *The Journal of Cell Biology*, *70*(1), 157-177.

Kolosov, D., Bui, P., Chasiotis, H., & Kelly, S. P. (2013). Claudins in teleost fishes. *Tissue Barriers*, *1*(3), e25391.

Kültz, D. (2015). Physiological mechanisms used by fish to cope with salinity stress. *Journal of Experimental Biology*, *218*(12), 1907-1914.

Krause, G., Protze, J., & Piontek, J. (2015). Assembly and function of claudins: Structure–function relationships based on homology models and crystal structures. *Seminars in Cell & Developmental Biology*, *42*, 3-12.

Laghaei, R., Yu, A. S., & Coalson, R. D. (2016). Water and ion permeability of a claudin model: A computational study. *Proteins: Structure, Function, and Bioinformatics*, *84*(3), 305-315.

Marshall, W. S., Katoh, F., Main, H. P., Sers, N., & Cozzi, R. R. F. (2008). Focal adhesion kinase and β1 integrin regulation of Na+, K+, 2Cl– cotransporter in osmosensing ion transporting cells of killifish, *Fundulus heteroclitus*. *Comparative Biochemistry and Physiology Part A: Molecular & Integrative Physiology*, *150*(3), 288-300.

Marshall, W. S., Watters, K. D., Hovdestad, L. R., Cozzi, R. R., & Katoh, F. (2009). CFTR Cl–channel functional regulation by phosphorylation of focal adhesion kinase at tyrosine 407 in osmosensitive ion transporting mitochondria rich cells of euryhaline killifish. *Journal of Experimental Biology*, *212*(15), 2365-2377.

Marshall, W. S., Breves, J. P., Doohan, E. M., Tipsmark, C. K., Kelly, S. P., Robertson, G. N., & Schulte, P. M. (2018). claudin-10 isoform expression and cation selectivity change with salinity in salt-secreting epithelia of *Fundulus heteroclitus*. *Journal of Experimental Biology*, *221*(1).

Mérette, D., Bourret, A., & Turgeon, J. (2009). Diversity and distribution of gynogenetic hybrids between *Fundulus diaphanus* and *Fundulus heteroclitus* in Porter's Lake (Nova Scotia) in relation to salinity. *Journal of Fish Biology*, *75*(5), 1115-1122.

McCormick, S. D., Farrell, A. P., & Brauner, C. J. (Eds.). (2013). *Fish Physiology: Euryhaline Fishes*, 32.

Osterberg, J. S., Cammen, K. M., Schultz, T. F., Clark, B. W., & Di Giulio, R. T. (2018). Genome-wide scan reveals signatures of selection related to pollution adaptation in non-model estuarine Atlantic killifish (*Fundulus heteroclitus*). *Aquatic Toxicology*, *200*, 73-82.

PureLink ™ Invitrogen protocols. Lachine Québec, Canada.

Reid, N. M., & Whitehead, A. (2015). Functional genomics to assess biological responses to marine pollution at physiological and evolutionary timescales: toward a vision of predictive ecotoxicology. *Briefings in Functional Genomics*, *15*(5), 358-364.

Schulte, P. M. (2007). Responses to environmental stressors in an estuarine fish: Interacting stressors and the impacts of local adaptation. *Journal of Thermal Biology*, *32*(3), 152-161.

Scott, G. R., Claiborne, J. B., Edwards, S. L., Schulte, P. M., & Wood, C. M. (2005). Gene expression after freshwater transfer in gills and opercular epithelia of killifish: insight into divergent mechanisms of ion transport. *Journal of Experimental Biology*, *208*(14), 2719-2729.

Suescún-Bolívar, L. P., & Thomé, P. E. (2015). Osmosensing and osmoregulation in unicellular eukaryotes. *World Journal of Microbiology and Biotechnology*, *31*(3), 435-443.

Suzuki, H., Tani, K., Tamura, A., Tsukita, S., & Fujiyoshi, Y. (2015). Model for the architecture of claudin-based paracellular ion channels through tight junctions. *Journal of Molecular Biology*, *427*(2), 291-297.

Taylor, S., Wakem, M., Dijkman, G., Alsarraj, M., & Nguyen, M. (2010). A practical approach to RT-qPCR—publishing data that conform to the MIQE guidelines. *Methods*, *50*(4), S1-S5.

Thermo Fisher Scientific GeneJET RNA Purification Kit protocols. Chelmsford MA, USA.

Tipsmark, C. K., Kiilerich, P., Nilsen, T. O., Ebbesson, L. O., Stefansson, S. O., & Madsen, S. S. (2008a). Branchial expression patterns of claudin isoforms in Atlantic

salmon during seawater acclimation and smoltification. *American Journal of Physiology-Regulatory, Integrative and Comparative Physiology*, 294(5), R1563-R1574.

Tipsmark, C. K., Luckenbach, J. A., Madsen, S. S., Kiilerich, P., & Borski, R. J. (2008b). Osmoregulation and expression of ion transport proteins and putative claudins in the gill of southern flounder (*Paralichthys lethostigma*). *Comparative Biochemistry and Physiology Part A: Molecular & Integrative Physiology*, *150*(3), 265-273.

Whitehead, A. (2010). The evolutionary radiation of diverse osmotolerant physiologies in killifish (*Fundulus* sp.). *Evolution: International Journal of Organic Evolution*, *64*(7), 2070-2085.

Zadunaisky, J. A. (1996). Chloride cells and osmoregulation. *Kidney International*, *49*(6), 1563-1567.